Development of highly performing water-adsorption chiller using new aluminophosphate as water adsorbent

Kanghee Cho, Sang Kyum Kim, Eunkyung Lee, Hyung-Chul Yoon, Jong-Nam Kim*

Korea Institute of Energy Research, 152 Gajeong-ro, Yuseong-gu, Daejeon 34129, Republic of Korea

Abstract

Adsorption chiller is a thermally operating refrigeration system. It uses water as refrigerant which is adsorbed and desorbed on solid adsorbents such as silica gel or zeolite. It has been considered and gaining great interest as an environment-friendly and energy-efficient system. Adsorption chiller utilizes low-temperature (below 90°C) renewable heat or waste heat to make cold water of below 15°C during the summer season. Many research institutes and companies (*e.g.*, Mycom, Nishiyodo, Mitsubishi Plastics, Zeopower, Invensor, SorTech etc.) have developed adsorption chillers. The key to the development of adsorption chillers that exhibit high efficiency and good performance is the development of suitable adsorbents that can adsorb as much refrigerant as possible at room temperature and desorb the refrigerant easily using low-temperature heat during the regeneration step. We have developed aluminophosphate-based water adsorbent which meets simultaneously two sides of requirements. In addition, we have designed and assembled water adsorption chiller system as compactly as possible. In this system, the aluminophosphate adsorbent was loaded as a bead-form or as coated on the fin-tube heat exchanger. Thus developed chiller was evaluated in comparison with previous adsorption-chiller, in the point of coefficient of performance (COP), specific cooling power and the compactness of entire system volume.

1. Introduction

Adsorption chiller is a type of refrigeration system, operating on the basic principle of heat removal by evaporation of liquid refrigerants (e.g., water, ammonia, and alcohol) and consequent adsorption in porous materials. Adsorption chiller systems have several advantages, including utilization of renewable heat, low electric capacity, and exclusion of Freon-gas-type refrigerants [1-2]. Many research institutes and private companies, including Mycom, Nishiyodo, Mitsubishi Plastics, Zeopower, Invensor, SorTech, and Shanghai Jiao Tong University, have developed adsorption chillers. The key to the development of adsorption chillers with high efficiency and good performance is the development of suitable adsorbents that can adsorb as much refrigerant as possible at room temperature and desorb the refrigerant easily using low-temperature heat during the regeneration step. In the case of an adsorption chiller that uses water as the refrigerant, nanoporous materials with high water uptake under 9 ~ 12 Torr at room temperature and with remarkable desorbing capability under 353 K are highly desirable for use in generating chilled water (~283 K). However, it is hard to control the chemical properties of the adsorbent materials in such a way as to achieve the desired performances in both sides. Furthermore, the feasibility of mass production and low production costs for the adsorbent are also required. Regular-density silica gel and zeolites have commonly been so far used as commercial water adsorbents in adsorption chiller systems [3-5].

In recent years, crystalline microporous aluminophosphates (referred to herein as $AlPO_4$ for brevity) has been attracting great interest as a water adsorbent in the application field of adsorption chillers [6-12]. These materials are normally synthesized under hydrothermal conditions, using alkyl amines or quaternary ammonium as micropore structure-directing agents. By changing the structure-directing agents, $AlPO_4$ has been synthesized with various pore structures (*e.g.*, AEL, AFI, CHA, and FAU) [13-17]. Additionally, under hydrothermal synthesis conditions, $AlPO_4$ containing various types of heteroatoms (e.g., Si, Fe, Mg, Cr, Co, and Mn) can easily be synthesized by the simple addition of heteroatom precursors to a synthesis gel [18-19]. In addition, $AlPO_4$ can easily be synthesized at low cost, and it has high thermal and hydrothermal stability [4,20-21].

From the perspective of application to adsorption chillers, $AlPO_4$ materials have somewhat weaker hydrophilicity than aluminosilicate-based zeolite [5,22-23] and therefore require less energy and milder conditions for the desorption–regeneration step. The Mitsubishi Chemical Company has produced the water-adsorbent products AQSOATM FAM-Z01, Z02, and Z05. These materials are $AlPO_4$-based microporous materials that contains small amounts of iron or silicon. FAM-Z01 exhibits water adsorption properties that are highly favorable for its application in adsorption chillers. Y.-D. Kim et al. reported that FAM-Z01 adsorbs approximately 0.19 g water/g adsorbent in the humidity range of 10–30% at 298 K, and the water could easily be desorbed at 343–353 K [6]. FAM-Z02 exhibits a higher water uptake capacity (~0.3 $g_{water} g_{adsorbent}^{-1}$), but most of the water is adsorbed at very low humidity levels, which means that FAM-Z02 requires more energy to regenerate [6,8]. Japan Mitsubishi Plastics invented an adsorption chiller using these AQSOATM water adsorbents that can generate 283 K cold water. Nevertheless, it has been desired to improve and to modify the $AlPO_4$-based water adsorbent to develop adsorption chiller with better performances.

Very recently, Cho et al. reported that the water adsorption properties of the $AlPO_4$ materials can be significantly changed by changing microporous structure and framework composition [24]. $AlPO_4$ containing CHA-type structure exhibits higher the amount of water uptake than $AlPO_4$ containing AFI-type structure, but the former requires higher desorption energy due to stronger water affinity than the latter. It was also mentioned that the water affinity can be finely tuned by adding inorganic or transition metal species (*e.g.*, Fe, Mg, Co and Cr) in the $AlPO_4$ frameworks. It was also possible to change water affinity impregnating hygroscopic inorganic salt such as calcium chloride in $AlPO_4$ materials. The resultant mixture is normally referred to composites salt in porous matrix (CSPMs). Based on this report, we have been trying to develop $AlPO_4$-based water adsorbent that is much more suitable to the application in adsorption chiller, by tuning structural or chemical properties of the $AlPO_4$ materials. Furthermore, we have studied on large scale synthesis of the $AlPO_4$ materials, granulation of the powder form $AlPO_4$ materials and coating $AlPO_4$ on the aluminum plate, for the application of the synthesized $AlPO_4$ materials in water adsorption chiller system. In this report, the results of large-scale synthesis of the $AlPO_4$, granulating and coating of the $AlPO_4$, and water adsorption analysis of the newly synthesized water adsorbent were shown in detail.

2. Experimentals

2.1. Synthesis of $AlPO_4s$

Aluminophosphate samples were synthesized following hydrothermal synthesis methods described in previous reports [24,25].

2.2. Preparation of $AlPO_4$-based CSPM ($CaCl_2$-impregnated $AlPO_4$)

Hygroscopic inorganic salt, calcium chloride ($CaCl_2$) was dissolved completely in distilled water, and the $CaCl_2$ solution was impregnated in AFI-type $AlPO_4$ and mesoporous AFI-type $AlPO_4$ via incipient wetness impregnation procedure. In typical, 0.5 g of $CaCl_2$ (Aldrich) was completely dissolved in 2 ml distilled water, and this $CaCl_2$ solution was impregnated in to 9.5 g of the AFI-type $AlPO_4$ samples. The $CaCl_2$-impregnated $AlPO_4$ samples were dried in 373 K convection oven for 2 h.

2.3. Structural characterization

X-ray diffraction (XRD) patterns were taken with a Rigaku Multiflex diffractometer equipped with CuKα radiation (40 kV, 40 mA). The N_2 adsorption isotherms were measured at the liquid nitrogen temperature with an ASAP 2020 (Micromeritics) volumetric adsorption analyzer and a Tristar II (Micromeritics). Scanning electron micrograph (SEM) images were obtained without a metal coating, operating Hitachi S-4800 at 2 kV.

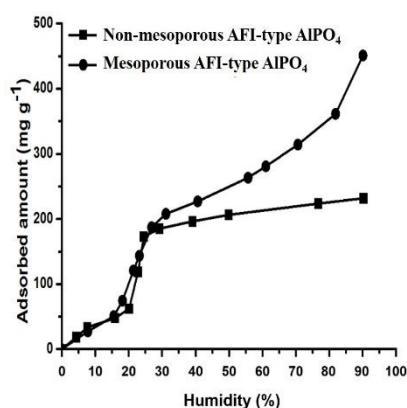*2.4. Characterization on water adsorption properties*

Fig. 1. Water sorption isotherms of AFI-type AlPO$_4$, taken at 308 K.

Water sorption isotherms of the various AlPO$_4$ samples were taken at 308 K at humidities from 0 to 100% using a BELSORP-aqua 3 volumetric sorption analyzer. Before the measurements were taken, the AlPO$_4$ samples were degassed at 423 K for 6 h under vacuum condition. Dynamic adsorption-desorption amount of AlPO$_4$ samples was evaluated subtracting the amount of adsorbed water under 12 Torr at 308 K (typical condition of adsorption step in water adsorption chiller system) by the amount of adsorbed water under 42 Torr at 348 K (typical condition of desorption step in water adsorption chiller system), where the amount of adsorbed water was measured by gravimetric instrument, DVS advantage (surface measurement systems). The conditions of adsorption and desorption can be easily converted in this measurement system.

3. Results and discussion

3.1. CaCl$_2$-impregnated AlPO$_4$

The AlPO$_4$ sample synthesized following previous method [24,25] was confirmed to have AFI-type crystalline microporous structure, and this contained small amount (5 mol% to total aluminum species) of iron species in the AlPO$_4$ framework. It contains 0.10 cm^3 g^{-1} of micropores and 0.02 cm^3 g^{-1} of mesopores, and exhibits 225 m^2 g^{-1} of BET external surface area. Another AlPO$_4$ sample synthesized following previous method [25], using organosilane surfactant was also confirmed to have AFI-type crystalline microporous structure. This sample contains 0.09 cm^3 g^{-1} of micropores and significant amount (0.31 cm^3 g^{-1}) of additional mesopores. Therefore, it could be refer this sample to mesoporous AFI-type AlPO$_4$. This sample shows 280 m^2 g^{-1} BET external surface area which is somewhat larger than that of non-mesoporous AFI-type AlPO$_4$ owing to the presence of mesopores.

The water adsorption properties of all of the AlPO$_4$ samples were measured at 308 K using a BELSORP-aqua 3 volumetric adsorption analyzer. Fig. 1 shows that the maximum amount of water uptake at 100% humidity (saturated pressure) was 0.22 g g^{-1} for the non-mesoporous AFI-type AlPO$_4$. Most of all water adsorption (0.18 g g^{-1}) was observed at humidity levels between 10% and 30% (12 Torr at 308 K). This AlPO$_4$ samples exhibited *S*-shape curves with steep increases at the aforementioned humidity level. Such a steep increase in the guest molecule uptake at a certain pressure is a typical characteristic of ordered porous materials and indicates that these AlPO$_4$ have micropores with quite uniform diameters. Fig. 1 also shows water adsorption isotherms of the mesoporous AFI AlPO$_4$ taken at 308 K. The mesoporous AFI AlPO$_4$ exhibited a slightly higher water adsorption (0.21 g g^{-1}) at low humidity levels (lower than 40%). More notably, the mesoporous AlPO$_4$ exhibited additional water uptake (0.24 g g^{-1}) at higher humidity (between 40% and 100%), in contrast to its solely microporous AlPO$_4$ counterpart which exhibited very little additional uptake (less than 0.02 g g^{-1}) in the same humidity range. According to the results of the pore analysis based on N$_2$ sorption (see Table 1), the mesoporous AFI AlPO$_4$ had a higher BET surface area (55 m^2 g^{-1}; 23% higher) and a greater pore volume (0.13 cm^3 g^{-1}; 100% higher) than its solely microporous counterpart. The larger amount of water adsorbed in the 40–100% humidity range could be attributed to the presence of mesopores. By correlating the water adsorption properties of the mesoporous AFI AlPO$_4$ with the pore texture determined by N$_2$ sorption analysis, we can explain the different water adsorption properties of mesoporous AlPO$_4$ as follows. At low humidity levels (lower t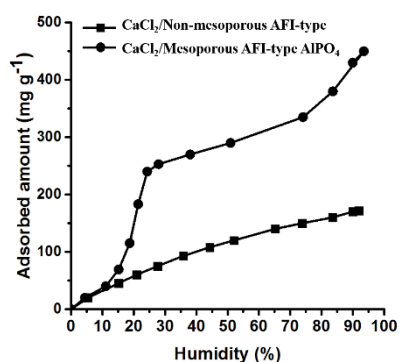han 40%), water uptake occurs in the forms of micropore filling and monolayer adsorption on mesopore surfaces. Therefore, mesoporous AlPO$_4$ exhibits a small increase in water uptake at low humidity levels because of the increased BET surface area. However, at high humidity levels (higher than 40%), the mesopore filling with water molecule can also occur. Therefore, mesoporous AlPO$_4$ exhibits a significant amount of additional water uptake at high relative humidity levels, in contrast to its bulk counterpart. The generation of mesopores in AlPO$_4$ affects the increase in the water uptake capacity, but almost all of the increase occurs at high relative humidity levels.

Fig. 2 shows that the water adsorption isotherms of non-mesoporous AFI AlPO$_4$ containing 5 wt% CaCl$_2$ and mesoporous AFI AlPO$_4$ counterpart. The non-mesoporous AFI-type AlPO$_4$ containing CaCl$_2$ exhibited 0.18 g g^{-1} of maximum water adsorption amount, but it

Fig. 2. Water sorption isotherms of AFI-type AlPO$_4$s containing CaCl$_2$, taken at 308 K.

exhibited only 0.05 g g^{-1} of water adsorption at humidity levels between 10% and 30%. The adsorption amount at this range was much decreased after impregnating CaCl$_2$. In the case of mesoporous AFI AlPO$_4$ containing CaCl$_2$, however, the amount of water adsorbed at same humidity range was 0.24 g g^{-1} which is somewhat increased owing to the impregnation of CaCl$_2$. The decrease of water adsorption amount in the case of non-mesoporous AFI AlPO$_4$ might be ascribed by the micropore blocking by CaCl$_2$ or by the coating of CaCl$_2$ on narrow external surfaces of the AlPO$_4$ crystal particles. In contrast, CaCl$_2$ is likely to be impregnated uniformly on the mesopore walls rather than blocking the micropores in the case of mesoporous AFI AlPO$_4$. It could be explained by the large external surfaces of the mesoporous AFI AlPO$_4$. Although it is necessary to find another evidence to explain clearly this phenomena, it is still quite interesting that the water adsorption amount at the humidity levels between 10% and 30% is significantly increased by simple impregnation of CaCl$_2$, especially in the case of AlPO$_4$ materials.

Fig. 3. Water sorption isotherms of AFI-type AlPO$_4$s containing various amount of iron, taken at 308 K.

3.2. Fine control of water adsorption properties of AlPO$_4$ materials

It was especially studied the effect of incorporating heteroatoms in the AlPO$_4$ framework, in order to find a way to control finely the adsorption properties of the AlPO$_4$ adsorbents. Fig. 3 shows water adsorption isotherms for AFI-type AlPO$_4$ materials containing various contents (0, 2.5, 5.0, and 10 mol% with respect to aluminum species) of iron species. The maximum water uptake capacities (0.25 g g^{-1}) of a series of iron-containing AlPOs at 100% humidity were quite similar, irrespective of the iron content. In the humidity range between 10% and 30%, three materials exhibited water uptakes of approximately 0.18 g g^{-1}. Such similar water adsorption capacities for the four AFI-type AlPO$_4$ samples, irrespective of their iron content, can be explained by their similar BET surface areas and similar micropore volumes. In this series of AFI-AlPO$_4$, almost all water adsorption occurred in the humidity range of 10% to 30%. However, the humidity corresponding to the inflection point of the S-curve gradually decreased with increasing iron content. This interesting tendency can be explained by an increase in hydrophilicity due to the addition of iron species to the AlPO$_4$ framework. Based on these results, we concluded that the water adsorption properties can be precisely controlled by incorporating different amounts of heteroatoms.
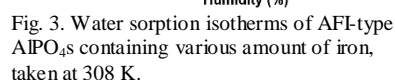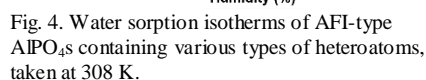
Fig. 4 shows a series of AFI-type AlPO$_4$ containing 5 mol% (with respect to aluminum species) of various heteroatoms (e.g., Fe, Mg, Cr, and Si) in an AlPO$_4$ framework. For comparison, the water adsorption isotherm of the AFI AlPO$_4$ without any heteroatom is also included. All the AlPO$_4$ exhibited similar maximum amounts of water uptakes (approximately 0.25 g g^{-1}) at less than 100% humidity. The water adsorption capacity is not significantly affected by changes in framework properties due to the incorporation of heteroatoms. This suggests that the maximum water uptake is closely related to micropore volume and the BET surface area of the sample (Table 1). The micropore volume and the BET surface areas of the samples with the same AFI microporous structures were not very different, irrespective of the types of heteroatoms incorporated. In addition, all the AlPO$_4$ samples exhibited S-shape curves with steep increases in the humidity range of 10–30%. However, the humidity at the inflection point varied slightly, depending on the type of heteroatoms incorporated. The humidity at the inflection point increased in the following order: Si- < Mg- < Fe- < Cr-impregnated < solely aluminophosphate. Among the AlPO$_4$ samples containing Mg, Fe, and Cr, the hydrophilicity of the AlPO$_4$ varied slightly different because of the different polarities and water affinities of the different types of heteroatoms. These results indicate that the magnesium species has a strong affinity for water and that the chromium species has a weak affinity for water. The silicon-impregnated AlPO$_4$ exhibited the strongest hydrophilicity. The reason for this is that the impregnation of silicon generates negative charges on neighboring aluminum atoms which has ionic interaction with water molecules. This ionic interaction is commonly stronger than polar–polar interaction.

Fig. 4. Water sorption isotherms of AFI-type AlPO$_4$s containing various types of heteroatoms, taken at 308 K.

Table 1. Porous texture properties of AFI-AlPO$_4$ samples.

	S_{BET}[a] (m^2 g^{-1})	V_{micro}[b] (cm^3 g^{-1})	V_{total}[c] (cm^3 g^{-1})	V_{meso}[d] (cm^3 g^{-1})
AFI-AlPO$_4$	231	0.10	0.11	0.01

AFI-Fe-AlPO$_4$	225	0.09	0.13	0.04
AFI-Cr-AlPO$_4$	255	0.11	0.15	0.04
AFI-Mg-AlPO$_4$	245	0.11	0.12	0.01
AFI-Si-AlPO$_4$	221	0.09	0.11	0.02
Mesoporous-AFI-AlPO$_4$	280	0.09	0.26	0.17

[a]S_{BET} (m^2 g^{-1})is BET surface area was calculated from edges obtained at relative pressure (P/P_0) between 0.05 and 0.3 of the isotherms using BET equation.
[b]V_{micro} is micropore volume calculated from Saito–Foley analysis.
[c]V_{total} is pore volume calculated at $P/P_0 = 0.95$
[d]V_{meso} is mesopore volume ($V_{total} - V_{micro}$)

3.3. Synthesis of new adsorbent exhibiting high dynamic adsorption-desorption performance

Fig. 5. Pictures of (a) powder-form and (b) granulized form of the synthesized adsorbent.

Based on the systematic study described in previous chapters, we have very recently synthesized new zeolite-derivatives-based adsorbent via hydrothermal synthesis route. It was also confirmed that this sample could be synthesized in large batch (kilogram-scale). The as-synthesized adsorbent was obtained in powder form. This powder form sample was confirmed to have certain crystalline ordered microporous structure from XRD analysis. The tap-density of this adsorbent powder was 0.64 g cm^{-3}. For the application of the newly synthesized adsorbent powder in adsorption chiller, we have tried to granulize the powder form to tiny beads with the diameter of 0.4 ~ 0.7 mm. Fig. 5 shows the picture of both powder form and granulized form of the synthesized adsorbent. The granulized beads of the sample are likely to have quite uniform shape and diameter. The tap density of this adsorbent beads was 0.65 g cm^{-3} which is quite similar to that of powder form. We could granulize this adsorbent in large scale (approximately, 1 kg). Furthermore, it was possible to adhere strongly the powder form of new adsorbent on aluminum plate using appropriate binder. The coating strength of the coated adsorbent was also measured. The picture of the adsorbent coating on aluminum plate and the characterization results will be presented in 12th HPC. It was quite notable that the water uptake capacity of our new adsorbent was well maintained after granulation or coating treatment, except for tiny decrease owing to decrease of partial weight of adsorbent in adsorbent/binder mixture. There was no evidence for pore blocking of new adsorbent by the used binder.
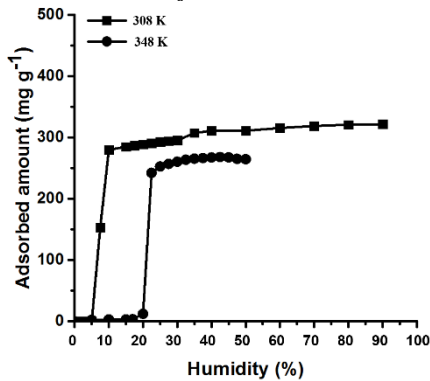

Fig. 6. Water sorption isotherms of our new adsorbent, taken at 308 K and 348 K.

Fig. 6 shows the water adsorption isotherms for the synthesized adsorbent, which were obtained at 308 K and 348 K. 308 K is normal temperature for adsorption step in adsorption chiller, and 348 K is slightly lower than normal temperature (353 ~ 373 K) for desorption/regeneration step in adsorption chiller. As shown in the water adsorption isotherm taken at 308 K, new adsorbent shows 0.33 g g^{-1} of maximum uptake amount under 100% of humidity level. Especially below the 30% of humidity level which is 12 Torr at 308 K and normal humidity for adsorption step in the adsorption chiller system, the adsorbent shows 0.31 g g^{-1} of the water uptake amount. That is, almost all water uptake occurred at very low humidity. In the case of the water adsorption isotherm taken at 348 K, the synthesized adsorbent exhibited 0.25 g g^{-1} of maximum water uptake, but most of all water adsorption occurred at the humidity level higher than 17% (50 Torr at 348 K). It is quite notable that this adsorbent exhibited almost negligible water uptake at 15% (42 Torr at 348 K) of humidity level which is typical condition for desorption step in adsorption chiller system. In other words, our new adsorbent adsorbed very small amount of water at desorption step, and it can desorb almost completely the adsorbed water at this condition during desorption-regeneration step in water adsorption chiller system. This characteristic of our new sample is significant merit when it used as water adsorbent in the chiller system. This sample can be easily regenerated using small amount of relatively low-temperature heat and it can increase adsorption-desorption efficiency and energy efficiency. Such a water adsorption properties of new adsorbent

including both high adsorption capacity and high regeneration efficiency are quite notable, as compared to other previously reported adsorbents.

For the more accurate evaluation of adsorption capability of new adsorbent during conversion between two adsorption and desorption step under real condition of water adsorption chiller system, gravimetric adsorption analyzer was used to measure the change of water adsorption amount of the adsorbent during changing adsorption conditions (temperature and humidity) between adsorption and desorption steps. The amount of water adsorbed in our new adsorbent was gravimetrically measured while the adsorption condition was dynamically converted between (12 Torr, 308 K for adsorption step) and (42 Torr, 348 K for desorption step). Fig. 7 shows the diagram exhibiting the change of temperature, humidity and the weight of the adsorbent sample with time on stream. The amount of water adsorbed in the adsorbent in adsorption step (12 Torr, 308 K) was 0.31 g g^{-1} but the amount of water adsorption in desorption step (42 Torr, 348 K) is almost negligible (~ 0.005 g g^{-1}). Thus the difference of water adsorption amount between two steps is approximately 0.30 g g^{-1}. This value is almost same as the value measured under 30% humidity at 308 K during obtaining water adsorption isotherm (see fig. 6). This result indicates that this new adsorbent can be regenerated by desorbing the adsorbed water almost completely during desorption step in the system. This adsorption capability was still maintained after 10 cycles of adsorption-desorption step-conversion. The present reported water adsorption properties of the new water adsorbent is quite notable, as comparing the water adsorption capability of previous zeolite- and alumino-phosphate-based adsorbents.
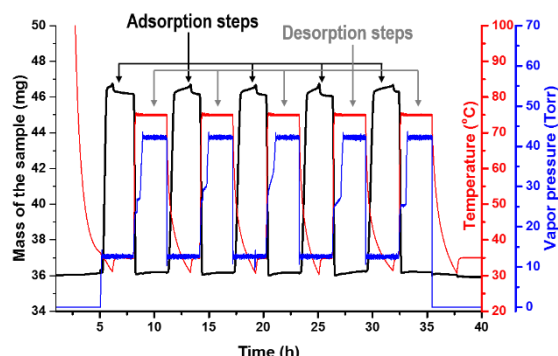

Fig. 7. Changes of temperature, humidity and the amount of adsorbed water, recorded with time on stream.

3.4. Installation of water adsorption chiller system using our new water adsorbent

As reported in several previous papers and patents, the water adsorption chiller system is normally assembled by several parts such as two adsorption chamber including water adsorbent, fin-type heat exchanger and water circulation pipes, water evaporation chamber, vapor condensation chamber, connecting pipes and valves. We have been assembling these parts to form entire system. It is on the progress to make optimized design of the system for maximizing energy efficiency and cooling efficiency. The final design and real picture of the adsorption chiller system will be presented in 2017 heat pump conference. Our new zeolite-derivative-based adsorbent which was synthesized in this work will be loaded in this adsorption chiller system, and water adsorption capability of the adsorbent under real condition and cooling efficiency will be measured soon. The detail results will be presented in the heat pump conference.

4. Conclusion

In this work, we focused on the possibility of developing new zeolite- or aluminophosphate-based adsorbents which shows high performance as water adsorbent in adsorption chiller system. For rational development of new adsorbent, systematic and fundamental studies on the effect of porous structure and the effect of physico-chemical properties of the aforementioned adsorbent to the water adsorption properties have been proceeded. From these systematic studies, it was confirmed that the water adsorption properties can be finely controlled by changing porous structure and the chemical composition of the adsorbent framework. Based on these studies, we have very recently developed new adsorbent exhibiting great performance as a water adsorbent in adsorption chiller system. In parallel, we have successfully done large-scale (kilogram-scale) synthesis of new adsorbent. It was also possible to granulize this adsorbent and to coat it on aluminum plate. We expected that we can develop adsorption chiller system exhibiting high energy-efficiency and cooling efficiency by using newly synthesized adsorbent in near future.

5. Acknowledgement

6. References

[1] F. Meunier, Special Issue Solid Sorption Refrigeration and Heat Pumps Solid sorption: An alternative to CFCs, Heat Recovery Systems and CHP, 13 (1993) 289-295.

[2] S.K. Fischer, J.J. Tomlinson, P.J. PHughes, Energy and global warming impacts of not-in-kind and next generation CFC and HCFC alternatives, Oak Ridge National Laboratory, 1994.

[3] F. Meunier, Theoretical performances of solid adsorbent cascading cycles using the zeolite-water and active carbon-methanol pairs: four case studies, Journal of Heat Recovery Systems, 6 (1986) 491-498.

[4] K.C. Ng, H.T. Chua, C.Y. Chung, C.H. Loke, T. Kashiwagi, A. Akisawa, B.B. Saha, Experimental investigation of the silica gel–water adsorption isotherm characteristics, Applied Thermal Engineering, 21 (2001) 1631-1642.

[5] F.B. Cortés, F. Chejne, F. Carrasco-Marín, A.F. Pérez-Cadenas, C. Moreno-Castilla, Water sorption on silica- and zeolite-supported hygroscopic salts for cooling system applications, Energy Conversion and Management, 53 (2012) 219-223.

[6] Y.-D. Kim, K. Thu, K.C. Ng, Adsorption characteristics of water vapor on ferroaluminophosphate for desalination cycle, Desalination, 344 (2014) 350-356.

[7] K. Inagaki, A. Kosaka, S. Inoue, Y. Aikawa, T. Takewaki, M. Yamazaki, H. Watanabe, H. Kakiuchi, M. Iwade, Adsorbent for heat utilization system, adsorbent for regenerator system, regenerator system comprising the adsorbent, ferroaluminophosphate and method for production thereof, US Patent 7,037,360, 2006.

[8] S. Shimooka, K. Oshima, H. Hidaka, T. Takewaki, H. Kakiuchi, A. Kodama, M. Kubota, H. Matsuda, The evaluation of direct cooling and heating desicant device coated with FAM, Journal of Chemical Engineering of Japan, 40 (2007) 1330-1334.

[9] M.J. Goldsworthy, Measurements of water vapour sorption isotherms for RD silica gel, AQSOA-Z01, AQSOA-Z02, AQSOA-Z05 and CECA zeolite 3A, Microporous and Mesoporous Materials, 196 (2014) 59-67.

[10] P.G. Youssef, S.M. Mahmoud, R.K. Al-Dadah, Performance analysis of four bed adsorption water desalination/refrigeration system, comparison of AQSOA-Z02 to silica-gel, Desalination, 375 (2015) 100-107.

[11] H. Kakiuchi, T. Takewaki, M. Fujii, M. Yamazaki, H. Takumi, H. Watanabe, K. Inagaki, A. Kosaka, S. Inoue, S. Inoue, Adsorption heat pump and use of adsorbent as adsorbent for adsorption heat pump, US Patent 8,333,079, 2012.

[12] H. Watanabe, T. Takewaki, M. Yamazaki, H. Kakiuchi, K. Inagaki, A. Kosaka, N. Hosokawa, Zeolite, process for producing the same, adsorbent comprising the zeolite, heat utilization system, adsorption heat pump, cold/heat storage system, and air-conditioning apparatus for humidity regulation, US Patent 7,527,777, 2009.

[13] I. Girnus, K. Jancke, R. Vetter, J. Richter-Mendau, J. Caro, Large AlPO4-5 crystals by microwave heating, Zeolites, 15 (1995) 33-39.

[14] S. Wilson, P. Barger, The characteristics of SAPO-34 which influence the conversion of methanol to light olefins, Microporous and Mesoporous Materials, 29 (1999) 117-126.

[15] A.M. Prakash, S. Unnikrishnan, Synthesis of SAPO-34: high silicon incorporation in the presence of morpholine as template, Journal of the Chemical Society, Faraday Transactions, 90 (1994) 2291-2296.

[16] U.S. Thakur, R. Tomar, Synthesis variables and behavior of VPI-5: A review, Microporous and Mesoporous Materials, 201 (2015) 258-270.

[17] M.J. Franco, J. Pérez-Pariente, A. Misud, T. Blasco, J. Sanz, Crystallization kinetics of SAPO-37, Zeolites, 12 (1992) 386-394.

[18] B.M. Weckhuysen, R.R. Rao, J. A. Martens, R.A. Schoonheydt, Transition Metal Ions in Microporous Crystalline Aluminophosphates: Isomorphous Substitution, European Journal of Inorganic Chemistry, 1999 (1999) 565-577.

[19] H.O. Pastore, S. Coluccia, L. Marchese, Porous Aluminophosphates :From Molecular Sieves to Designed Acid Catalysts, Annual Review of Materials Research, 35 (2005) 351-395.

[20] Y.I. Aristov, G. Restuccia, G. Cacciola, V.N. Parmon, A family of new working materials for solid sorption air conditioning systems, Applied Thermal Engineering, 22 (2002) 191-204.

[21] F. Jeremias, D. Frohlich, C. Janiak, S.K. Henninger, Water and methanol adsorption on MOFs for cycling heat transformation processes, New Journal of Chemistry, 38 (2014) 1846-1852.

[22] A.O. Dieng, R.Z. Wang, Literature review on solar adsorption technologies for ice-making and air-conditioning purposes and recent developments in solar technology, Renewable and sustainable energy reviews, 5 (2001) 313-342.

[23] S.K. Henninger, G. Munz, K.F. Ratzsch, P. Schossig, Cycle stability of sorption materials and composites for the use in heat pumps and cooling machines, Renewable Energy, 36 (2011) 3043-3049.

[24] K. Cho, S.K. Kim, E.K. Lee, J.-N. Kim, Fine control of water-adsorption properties of crystalline microporous aluminophosphates by changing porous structure and framework composition for application in water adsorption chiller, Journal of Nanoscience and Nanotechnology, 17 (2017) (doi: 10.1166/jnn.2017.13838).

[25] M. Choi, R. Srivastava, R. Ryoo, Organosilane surfactant-directed synthesis of mesoporous aluminophosphates constructed with crystalline microporous frameworks, Chemical Communications, (2006) 4380-4382.